Proceedings of the ASME 2011 International Design Engineering Technical Conferences & Computers and Information in Engineering Conference
IDETC/CIE 2011
August 28-31, 2011, Washington, DC, USA

DETC2011-47705

MODAL ANALYSIS OF JOINTED STRUCTURES

D. Dane Quinn*
Department of Mechanical Engineering
The University of Akron
Akron, Ohio 44325–3903

ABSTRACT

Structural systems are often composed of multiple components joined together at localized interfaces. Compared to a corresponding monolithic system, these interfaces are designed to leave the load carrying capability of the system unchanged and the resulting effect on the system stiffness is minimal. Hence the mode shapes and frequencies of the dominant structural modes are relatively insensitive to the presence of the interfaces. However, the energy dissipation in such systems is strongly dependent on the joints. The microslip that occurs at each interface couples together the structural modes of the system and introduces nonlinear damping into the system, effectively altering the observed damping of the structural modes. This work develops equations of motion for a jointed structure in terms of the structural modal coordinates and implements a reduced-order description of the microslip that occurs at the interface between components. The interface is incorporated into the modal description of the system through an existing decomposition of a series-series Iwan interface model and a continuum approximation for microslip of a elastic rod. The developed framework is illustrated through a discrete three degree-of-freedom system.

1 INTRODUCTION

Complex engineering structures are typically composed of multiple components, connected by mechanical interfaces such as bolted joints and/or threaded connections. These connections are designed so as not to alter the stiffness and load carrying capacity of the structure as compared to a monolithic version. However, these interfaces often contribute significantly to the overall observed dissipation in the dynamical response of such structures [1–3] and introduces nonlinear behavior into the structural response that can be observed both experimentally [4, 5] and in detailed finite element calculations [6, 7]. This interfacial damping typically arises from microslip, that is, rough sliding contact which occurs over a small spatial interval. This localized phenomena is distinct from macroslip, whereby the entire interface undergoes slip.

Unfortunately, when modeling microslip even the incorporation of simple friction laws, such as Coulomb friction, into larger computational models is problematic. As the length scale of the computational model is reduced to resolve the interface and the region of microslip, the corresponding time scale for the simulation is reduced accordingly. Thus, when a simulation of specified time duration is required, the computational effort can grow unacceptably large [8, 9]. To overcome these computational limitations, simulations often introduce non-physical damping that can be easily incorporated into the model (e.g., the use of proportional damping), and then identify the damping parameters to match experimentally observed results [6, 10]. However, this approach significantly constrains the true predictive capability of the simulation. For different loading levels or operational conditions, one must first determine the appropriate damping parameters to match available observations.

*quinn@uakron.edu

Recently, a number of models for the interface have been developed with the goal of reducing the computational load that occurs with the introduction of the interface. Representations for the dissipation induced by the interface have been developed based on, for example, collections of discrete Jenkins elements or Iwan models [11–16] or other hysteretic laws [14, 17, 18].

Despite the presence of the interface, the response of a typical structure is still well-described by the linear structural modal frequencies and mode shapes. While the coupling between modes due to the interface (absent in the linear monolithic component) is minor, the nonlinear damping introduced by the interface alters the decay of these modes. This work develops the structural equations of motion for jointed structures in terms of modal coordinates, and identifies a reduced-order model for the interfacial damping that can be incorporated into this framework. In the context of interface damping, the idea of a modal description of the structural equations of motion has recently been described by Segalman [19]. The damping was then postulated to give rise to a decoupled set of modal equations in which each mode was subject to a parallel-series Iwan model to describe the presence of the joint. In contrast, the current paper describes the deformation across the the joint exactly in terms of the modal coordinates and then relates this back to the modal forces in the modal equations of motion, based on work by Miller and Quinn [20] and Quinn and Segalman [13].

2 MODAL ANALYSIS OF JOINTED STRUCTURES

We consider a general jointed structure as shown in Figure 1, consisting of two components, $\mathcal{C}_1$ and $\mathcal{C}_2$, which overlap in a region $\mathcal{J}$ containing an interface. Thus we identify three regions $\hat{\mathcal{C}}_1$, $\hat{\mathcal{C}}_2$, and $\mathcal{J}$, where

$$\hat{\mathcal{C}}_1 = \mathcal{C}_1 - \mathcal{J}, \qquad \hat{\mathcal{C}}_2 = \mathcal{C}_2 - \mathcal{J}. \tag{1}$$

In this, it is assumed that the regions $\hat{\mathcal{C}}_1$ and $\hat{\mathcal{C}}_2$ are not adjacent. Instead they are separated by the region $\mathcal{J}$. Moreover, the region $\mathcal{J}$ is not taken to be the physical interface, but instead contains the interface. Thus the boundary of $\mathcal{J}$ is located at some distance away from the physical interface.

In addition, consider a monolithic structure $\mathcal{M}$ as the union of $\mathcal{C}_1$ and $\mathcal{C}_2$. The region of overlap no longer contains an interface and is instead denoted as $\mathcal{K}$. Note that $\mathcal{J}$ and $\mathcal{K}$ are identical in terms of physical extent, differing only in the presence of the interface.

2.1 Monolithic Structure

The monolithic structure is assumed to be linear and undamped, with its deformation over $\mathcal{M}$ governed by the equation of motion

Figure 1: Jointed structure; components $\mathcal{C}_1$ and $\mathcal{C}_2$ overlap in the region $\mathcal{J}$.

$$\mathbf{M}_{\mathcal{M}}\,\ddot{\mathbf{u}} + \mathbf{K}_{\mathcal{M}}\,\mathbf{u} = \mathbf{0}. \tag{2}$$

The above monolithic structure, subject to specified boundary conditions, admits a modal decomposition with modal functions $\boldsymbol{\phi}_j$, so that

$$\mathbf{u}(t) = \sum_{j=1}^{\infty} A_j(t)\,\boldsymbol{\phi}_j. \tag{3}$$

The equation of motion for each mode can therefore be obtained as

$$\left(\boldsymbol{\phi}_i^T\,\mathbf{M}_{\mathcal{M}}\,\boldsymbol{\phi}_i\right)\,\ddot{A}_i + \left(\boldsymbol{\phi}_i^T\,\mathbf{K}_{\mathcal{M}}\,\boldsymbol{\phi}_i\right)\,A_i = 0, \tag{4}$$

where ϕ_i is the i^{th} mode shape for the monolithic structure obtained by solving the standard eigenvalue problem from structural analysis.

Note that the integral over the domain $\mathcal{M}$ can be split over each of the subdomains identified above, so that

$$\mathcal{M} = \hat{\mathcal{C}}_1 + \mathcal{K} + \hat{\mathcal{C}}_2. \tag{5}$$

where the mass and stiffness matrices can be decomposed over each of the three regions as

$$\begin{bmatrix} \mathbf{M}_{\hat{\mathcal{C}}_1} & \mathbf{0} & \mathbf{0} \\ \mathbf{0} & \mathbf{M}_{\mathcal{K}} & \mathbf{0} \\ \mathbf{0} & \mathbf{0} & \mathbf{M}_{\hat{\mathcal{C}}_2} \end{bmatrix} \begin{bmatrix} \ddot{\mathbf{u}}_{\hat{\mathcal{C}}_1} \\ \ddot{\mathbf{u}}_{\mathcal{K}} \\ \ddot{\mathbf{u}}_{\hat{\mathcal{C}}_2} \end{bmatrix} + \begin{bmatrix} \mathbf{K}_{\hat{\mathcal{C}}_1} & \mathbf{0} & \mathbf{0} \\ \mathbf{0} & \mathbf{K}_{\mathcal{K}} & \mathbf{0} \\ \mathbf{0} & \mathbf{0} & \mathbf{K}_{\hat{\mathcal{C}}_2} \end{bmatrix} \begin{bmatrix} \mathbf{u}_{\hat{\mathcal{C}}_1} \\ \mathbf{u}_{\mathcal{K}} \\ \mathbf{u}_{\hat{\mathcal{C}}_2} \end{bmatrix} + \begin{bmatrix} \mathbf{T}_{1\mathcal{K}} & \mathbf{T}_{\mathcal{K}1} & \mathbf{0} \\ -\mathbf{T}_{1\mathcal{K}} & -\mathbf{T}_{\mathcal{K}1} - \mathbf{T}_{\mathcal{K}2} & -\mathbf{T}_{2\mathcal{K}} \\ \mathbf{0} & \mathbf{T}_{\mathcal{K}2} & \mathbf{T}_{2\mathcal{K}} \end{bmatrix} \begin{bmatrix} \mathbf{u}_{\hat{\mathcal{C}}_1} \\ \mathbf{u}_{\mathcal{K}} \\ \mathbf{u}_{\hat{\mathcal{C}}_2} \end{bmatrix} = \mathbf{0} \tag{6}$$

Here the monolithic mass matrix $\mathbf{M}_{\mathcal{M}}$ has been decomposed into a block diagonal component over each of the subdomains, so that there is no mass coupling between the components. Likewise, the stiffness $\mathbf{K}_{\mathcal{M}}$ has been decomposed into a block diagonal component together with a second component $\mathbf{T}$, where the stiffness components $\mathbf{T}_{ij}$ describe

the coupling between the exterior regions $\hat{\mathcal{C}}_1$ and $\hat{\mathcal{C}}_2$ and the region $\mathcal{K}$. Recall that the $\mathcal{K}$ represents the region in the monolithic structure that corresponds to the interface region $\mathcal{J}$ in the jointed structure. Thus in the monolithic structure the contact forces $\boldsymbol{Q}^{\mathcal{K}}$ between the regions can be represented as

$$\begin{bmatrix} \boldsymbol{Q}_1^{\mathcal{K}} \\ -\boldsymbol{Q}_1^{\mathcal{K}} - \boldsymbol{Q}_2^{\mathcal{K}} \\ \boldsymbol{Q}_2^{\mathcal{K}} \end{bmatrix} = \begin{bmatrix} \mathbf{T}_{1\mathcal{K}} & \mathbf{T}_{\mathcal{K}1} & \mathbf{0} \\ -\mathbf{T}_{1\mathcal{K}} & -\mathbf{T}_{\mathcal{K}1} + \mathbf{T}_{\mathcal{K}2} & -\mathbf{T}_{2\mathcal{K}} \\ \mathbf{0} & \mathbf{T}_{\mathcal{K}2} & \mathbf{T}_{2\mathcal{K}} \end{bmatrix} \begin{bmatrix} \mathbf{u}_{\hat{\mathcal{C}}_1} \\ \mathbf{u}_{\mathcal{K}} \\ \mathbf{u}_{\hat{\mathcal{C}}_2} \end{bmatrix} \quad (7)$$

Finally, the mode shapes can be decomposed over these regions as well, so that

$$\boldsymbol{\phi}_{\mathcal{M}} = \begin{bmatrix} \boldsymbol{\phi}_{\hat{\mathcal{C}}_1} & \boldsymbol{\phi}_{\mathcal{K}} & \boldsymbol{\phi}_{\hat{\mathcal{C}}_2} \end{bmatrix}^T \quad (8)$$

With this, the modal equations of motion over each region can be expressed as

$$\boldsymbol{\phi}_{\hat{\mathcal{C}}_1,i}^T \left\{ \left(\sum_{j=1}^{N} \mathbf{M}_{\hat{\mathcal{C}}_1} \boldsymbol{\phi}_{\hat{\mathcal{C}}_1,j} \ddot{A}_j \right) + \left(\sum_{j=1}^{N} \mathbf{K}_{\hat{\mathcal{C}}_1} \boldsymbol{\phi}_{\hat{\mathcal{C}}_1,j} A_j \right) \right\} = -\boldsymbol{\phi}_{\hat{\mathcal{C}}_1,i}^T \boldsymbol{Q}_1^{\mathcal{K}}, \quad (9)$$

$$\boldsymbol{\phi}_{\mathcal{K},i}^T \left\{ \left(\sum_{j=1}^{N} \mathbf{M}_{\mathcal{K}} \boldsymbol{\phi}_{\mathcal{K},j} \ddot{A}_j \right) + \left(\sum_{j=1}^{N} \mathbf{K}_{\mathcal{K}} \boldsymbol{\phi}_{\mathcal{K},j} A_j \right) \right\} = \boldsymbol{\phi}_{\mathcal{K},i}^T \left(\boldsymbol{Q}_1^{\mathcal{K}} + \boldsymbol{Q}_2^{\mathcal{K}} \right), \quad (10)$$

$$\boldsymbol{\phi}_{\hat{\mathcal{C}}_2,i}^T \left\{ \left(\sum_{j=1}^{N} \mathbf{M}_{\hat{\mathcal{C}}_2} \boldsymbol{\phi}_{\hat{\mathcal{C}}_2,j} \ddot{A}_j \right) + \left(\sum_{j=1}^{N} \mathbf{K}_{\hat{\mathcal{C}}_2} \boldsymbol{\phi}_{\hat{\mathcal{C}}_2,j} A_j \right) \right\} = -\boldsymbol{\phi}_{\hat{\mathcal{C}}_2,i}^T \boldsymbol{Q}_2^{\mathcal{K}}, \quad (11)$$

Combining Eqs. (9) and (11) yields

$$\begin{aligned} &\boldsymbol{\phi}_{\hat{\mathcal{C}}_1,i}^T \left\{ \left(\sum_{j=1}^{N} \mathbf{M}_{\hat{\mathcal{C}}_1} \boldsymbol{\phi}_{\hat{\mathcal{C}}_1,j} \ddot{A}_j \right) + \left(\sum_{j=1}^{N} \mathbf{K}_{\hat{\mathcal{C}}_1} \boldsymbol{\phi}_{\hat{\mathcal{C}}_1,j} A_j \right) \right\} \\ &+ \boldsymbol{\phi}_{\hat{\mathcal{C}}_2,i}^T \left\{ \left(\sum_{j=1}^{N} \mathbf{M}_{\hat{\mathcal{C}}_2} \boldsymbol{\phi}_{\hat{\mathcal{C}}_2,j} \ddot{A}_j \right) + \left(\sum_{j=1}^{N} \mathbf{K}_{\hat{\mathcal{C}}_2} \boldsymbol{\phi}_{\hat{\mathcal{C}}_2,j} A_j \right) \right\} \\ &= -\boldsymbol{\phi}_{\hat{\mathcal{C}}_1,i}^T \boldsymbol{Q}_1^{\mathcal{K}} - \boldsymbol{\phi}_{\hat{\mathcal{C}}_2,i}^T \boldsymbol{Q}_2^{\mathcal{K}}, \end{aligned} \quad (12)$$

The right hand side of Eq. (12) represents the influence of the region of overlap $\mathcal{K}$ on the overall monolithic structure $\mathcal{M}$ in the regions $\hat{\mathcal{C}}_1$ and $\hat{\mathcal{C}}_2$. In general the contact forces $Q_i^{\mathcal{K}}(t)$ must be determined appropriately to describe this (monolithic) region of the structure. Specifically, the right hand side of these equations of motion is not decoupled, that is, the i^{th} equation possibly depends on each modal amplitude A_j, $j = 1, \ldots, N$. It is only with the inclusion of the appropriate contact forces $\boldsymbol{Q}^{\mathrm{K}}$ that the resulting equations decouple into the familiar modal form (c.f. Eq. (4)).

2.2 Jointed Structure

Now turning to the jointed structure, Eq. (12) is still valid, provided $Q_i^{\mathcal{K}}(t)$ is replaced by the appropriate contact force arising within the jointed structure, defined as $Q_i^{\mathcal{J}}(t)$. The contact forces of the jointed and monolithic structure can be related as

$$\boldsymbol{Q}_i^{\mathcal{J}}(t) = \boldsymbol{Q}_i^{\mathcal{K}}(t) + \boldsymbol{\delta Q}_i(t), \quad (13)$$

Thus the term $\boldsymbol{\delta Q}_i$ characterizes the deviation in the contact force of the jointed structure at the boundary between $\hat{\mathcal{C}}_i$ and $\mathcal{K}$, as compared to that of the corresponding monolithic structure. These equations of motion become

$$\begin{aligned} &\boldsymbol{\phi}_{\hat{\mathcal{C}}_1,i}^T \left\{ \left(\sum_{j=1}^{N} \mathbf{M}_{\hat{\mathcal{C}}_1} \boldsymbol{\phi}_{\hat{\mathcal{C}}_1,j} \ddot{A}_j \right) + \left(\sum_{j=1}^{N} \mathbf{K}_{\hat{\mathcal{C}}_1} \boldsymbol{\phi}_{\hat{\mathcal{C}}_1,j} A_j \right) \right\} \\ &+ \boldsymbol{\phi}_{\hat{\mathcal{C}}_2,i}^T \left\{ \left(\sum_{j=1}^{N} \mathbf{M}_{\hat{\mathcal{C}}_2} \boldsymbol{\phi}_{\hat{\mathcal{C}}_2,j} \ddot{A}_j \right) + \left(\sum_{j=1}^{N} \mathbf{K}_{\hat{\mathcal{C}}_2} \boldsymbol{\phi}_{\hat{\mathcal{C}}_2,j} A_j \right) \right\} \\ &= -\boldsymbol{\phi}_{\hat{\mathcal{C}}_1,i}^T \left(\boldsymbol{Q}_1^{\mathcal{K}}(t) + \boldsymbol{\delta Q}_1(t) \right) - \boldsymbol{\phi}_{\hat{\mathcal{C}}_2,i}^T \left(\boldsymbol{Q}_1^{\mathcal{K}}(t) + \boldsymbol{\delta Q}_1(t) \right). \end{aligned} \quad (14)$$

Making use of Eqs. (4), (10), and (5), the equations of motion for the jointed structure can be written as

$$\begin{aligned} &\left(\boldsymbol{\phi}_i^T \mathbf{M}_{\mathcal{M}} \boldsymbol{\phi}_i \right) \ddot{A}_i + \left(\boldsymbol{\phi}_i^T \mathbf{K}_{\mathcal{M}} \boldsymbol{\phi}_i \right) A_i \\ &\qquad = \boldsymbol{\phi}_{\mathcal{K},i}^T \left(\boldsymbol{\delta Q}_1(t) + \boldsymbol{\delta Q}_2(t) \right) \\ &\qquad\quad - \left(\boldsymbol{\phi}_{\hat{\mathcal{C}}_1,i}^T \boldsymbol{\delta Q}_1(t) + \boldsymbol{\phi}_{\hat{\mathcal{C}}_2,i}^T \boldsymbol{\delta Q}_2(t) \right). \end{aligned} \quad (15)$$

Here the left-hand side of the equations is the familiar modal equations for the structure. The right-hand side represents the effect of the isolated interface, which is incorporated through the terms $\boldsymbol{\delta Q}_1$ and $\boldsymbol{\delta Q}_2$. Note that the modal functions $\boldsymbol{\phi}_i$ are defined over the entire monolithic structure. Thus, this approach is not considered as a component mode synthesis, where the interface might exist at the boundary of the individual components. Rather, the joint is accounted for as an internal feature of the component.

This approach allows for the straightforward incorporation of isolated effects into the equations of motion, as written in terms of the linear mode shapes of the structure. While the equations of motion can be written in terms of any complete set of coordinates, the compact representation of the isolated forces described above is a distinguishing feature of this approach. Moreover, provided the terms $\boldsymbol{\delta Q}_1$ and $\boldsymbol{\delta Q}_2$ can be identified, this approach can be applied to any localized effects, including for example isolated nonlinearities [9]. If the isolated force is known in terms of the system coordinates, then this approach leads to the exact equations of motion. In addition, by expressing these equations in terms of the linear modal coordinates, this provides an appropriate beginning for model reduction techniques. The ability of this approach to describe the response of a general jointed structure depends on how well the assumed constitutive law describing $\boldsymbol{\delta Q}_i$ represents the contribution from the interfacial forces in the actual model (c.f., Eq. (13)). This places particular importance on the identification of the region $\mathcal{J}$ containing the joint. This region must be large enough to contain the interface, but allow for an accurate representation of the contact force.

2.3 Example: Discrete Linear Damping.

As an illustrative example, we consider a discrete three degree-of-freedom system with a single linear damper located between masses 2 and 3, as shown in Figure 2. In this example, each mass m and stiffness k are assumed to be identical. In the absence of damping ($b = 0$) the eigenpairs $(\omega_i^2, \mathbf{u}_i)$ and modal equations of motion can be written as

$$\left(\omega_1^2 = (2-\sqrt{2})\,\frac{k}{m}, \quad \boldsymbol{\phi}_1 = \left[\begin{array}{ccc} 1 & \sqrt{2} & 1 \end{array}\right]^T\right) \qquad m\,\ddot{A}_1 + (2-\sqrt{2})\,k\,A_1 = 0, \quad \text{(16a)}$$

$$\left(\omega_2^2 = 2\,\frac{k}{m}, \quad \boldsymbol{\phi}_2 = \left[\begin{array}{ccc} 1 & 0 & -1 \end{array}\right]^T\right) \qquad m\,\ddot{A}_2 + 2\,k\,A_2 = 0, \quad \text{(16b)}$$

$$\left(\omega_3^2 = (2+\sqrt{2})\,\frac{k}{m}, \quad \boldsymbol{\phi}_3 = \left[\begin{array}{ccc} 1 & -\sqrt{2} & 1 \end{array}\right]^T\right) \qquad m\,\ddot{A}_3 + (2+\sqrt{2})\,k\,A_3 = 0. \quad \text{(16c)}$$

In the above formulation, the first component $\hat{\mathcal{C}}_1$ is identified with masses 1 and 2, while the second component $\hat{\mathcal{C}}_2$ is identified with mass 3, so that, for example

$$\boldsymbol{\phi}_{\hat{\mathcal{C}}_1,1} = \left[\begin{array}{cc} 1 & \sqrt{2} \end{array}\right]^T, \quad \boldsymbol{\phi}_{\hat{\mathcal{C}}_2,1} = \left[\begin{array}{c} 1 \end{array}\right]^T. \qquad (17)$$

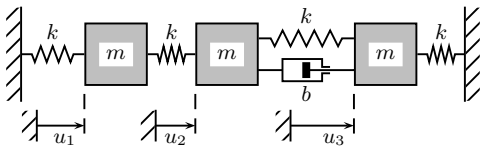

Figure 2: Discrete structure with damping.

Also, the damping force between masses 2 and 3 lead to interface forces of the form

$$\delta Q = b\,(\dot{u}_3 - \dot{u}_2), \quad \longrightarrow \qquad \boldsymbol{\delta Q}_1 = \left[\begin{array}{ccc} 0 & \delta Q \end{array}\right]^T, \quad \boldsymbol{\delta Q}_2 = \left[\begin{array}{c} -\delta Q \end{array}\right]^T. \quad (18)$$

Therefore, for the first modal equation

$$-\left(\boldsymbol{\phi}_{\hat{\mathcal{C}}_1,1}\,\boldsymbol{\delta Q}_1 + \boldsymbol{\phi}_{\hat{\mathcal{C}}_2,1}\,\boldsymbol{\delta Q}_2\right) = -\left((\sqrt{2}-1)\,b\,(\dot{u}_2 - \dot{u}_3)\right), \quad (19)$$

and

$$-\left(\boldsymbol{\phi}_{\hat{\mathcal{C}}_1,2}\,\boldsymbol{\delta Q}_1 + \boldsymbol{\phi}_{\hat{\mathcal{C}}_2,2}\,\boldsymbol{\delta Q}_2\right) = -\left(b\,(\dot{u}_2 - \dot{u}_3)\right), \quad (20)$$

$$-\left(\boldsymbol{\phi}_{\hat{\mathcal{C}}_1,3}\,\boldsymbol{\delta Q}_1 + \boldsymbol{\phi}_{\hat{\mathcal{C}}_2,3}\,\boldsymbol{\delta Q}_2\right) = -\left((\sqrt{2}+1)\,b\,(\dot{u}_3 - \dot{u}_2)\right). \quad (21)$$

In terms of the modal amplitudes the physical coordinates can be written as

$$u_1 = A_1 + A_2 + A_3, \quad u_2 = \sqrt{2}\,A_1 - \sqrt{2}\,A_3, \quad u_3 = A_1 - A_2 + A_3. \qquad (22)$$

Finally, in matrix form the damped equations of motion become

$$m\begin{bmatrix} 1 & 0 & 0 \\ 0 & 1 & 0 \\ 0 & 0 & 1 \end{bmatrix}\begin{bmatrix} \ddot{A}_1 \\ \ddot{A}_2 \\ \ddot{A}_3 \end{bmatrix} + b\begin{bmatrix} (\sqrt{2}-1)^2 & (\sqrt{2}-1) & -1 \\ (\sqrt{2}-1) & 1 & -(\sqrt{2}+1) \\ -1 & -(\sqrt{2}+1) & (\sqrt{2}+1)^2 \end{bmatrix}\begin{bmatrix} \dot{A}_1 \\ \dot{A}_2 \\ \dot{A}_3 \end{bmatrix} + k\begin{bmatrix} 2-\sqrt{2} & 0 & 0 \\ 0 & 2 & 0 \\ 0 & 0 & 2+\sqrt{2} \end{bmatrix}\begin{bmatrix} A_1 \\ A_2 \\ A_3 \end{bmatrix} = \mathbf{0}. \quad (23)$$

While the mass and stiffness matrix remain diagonal, the damping now fully couples each mode of the system, allowing for energy to be not only dissipated but dispersed throughout the modes of the structure. Note that while this example essentially describes a simple change of variables from physical to modal coordinates in the damped system, it serves to illustrate the methodology. In what follows, this methodology is combined with a novel description of the interface forces $\boldsymbol{\delta Q}_i$ to develop a description of the equations of motion for jointed structures.

3 DISTRIBUTED INTERFACE

We again consider the three degree-of-freedom system described above, but in the presence of a mechanical joint. The modal equations of motion for the monolithic structure are identical to those listed in Eq. (16), and the presence of a distributed interface can be incorporated in a straightforward manner provided the contact forces $\boldsymbol{\delta Q}_i$ are identified appropriately. For this system, the contact forces can be expressed as

$$\begin{gathered} \boldsymbol{Q}_1^{\mathcal{J}} = \left[\begin{array}{cc} 0 & Q^{\mathcal{J}} \end{array}\right]^T, \quad \boldsymbol{Q}_2^{\mathcal{J}} = \left[\begin{array}{c} -Q^{\mathcal{J}} \end{array}\right]^T, \\ Q^{\mathcal{J}} = Q^{\mathcal{K}} + \delta Q. \end{gathered} \tag{24}$$

Previous work by Miller and Quinn [20] studied a two-sided interface model for the response of a one-dimensional joint to external loading. The resulting model allowed for a decoupling of the elastic and dissipative effects. The elastic component of this model is equivalent to the monolithic structure while the dissipative component reduces to a discrete series-series Iwan model. In Quinn and Segalman [13], the dissipative properties of this Iwan model were analyzed and in the continuum limit the dissipation of the interface is equivalent to that of an elastic rod sliding on a rough, rigid foundation. From this, in the continuum limit the response of the dissipative component to general loading conditions can be developed in terms of the response to unidirectional loading of the undeformed rod, identified as $F = g(x)$. Following Masing's hypothesis [21], if this unidirectional loading curve is known, upon reversal of the loading direction the force evolution follows

$$F(x) = F^\star - 2\,\sigma^\star\, g\left(\frac{x - x^\star}{2\,\sigma^\star}\right), \tag{25}$$

where the displacement and loading at the reversal point is identified as $x^\star$ and $F^\star$ respectively and $\sigma^\star$ indicates the sign of the loading direction. A representative hysteresis curve for cyclic loading is shown in Figure 3. Note that the initial tangent stiffness of this system is infinite, as is the tangent stiffness upon load reversal.

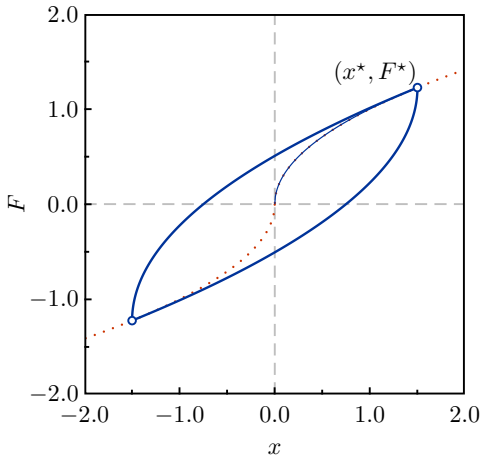

Figure 3: Illustrative hysteresis curve for cyclic loading. The unidirectional loading curve is shown dotted.

In terms of the monolithic component, the contact force is assumed to be

$$Q^{\mathcal{K}} = k\,\Delta, \tag{26}$$

where Δ is the displacement across the interface and k represents the equivalent stiffness of the interface. In addition, for the joint model of Miller and Quinn, we find that

$$Q^{\mathcal{J}} = g(\xi) = k\,w, \quad \Delta = w + \xi, \tag{27}$$

where w and ξ are internal displacements associated with the elastic and dissipative components respectively and $g(\xi)$ is the unidirectional loading curve described above. Note that the force across each of these decomposed elements is identical and the total displacement Δ equals the sum of the individual component displacements, so that they can be considered to be in series, as illustrated in Figure 4. From this constitutive model for the interface

$$g(\xi) = k\,(\Delta - \xi). \tag{28}$$

In addition, using Eq. (13) one finds that $\delta Q = -k\,\xi$ (c.f., Eq. (18)). Finally, combining these expressions

$$g\left(-\frac{\delta Q}{k}\right) = k\,\Delta + \delta Q. \tag{29}$$

Solving for δQ describes the unidirectional loading curve of the interface, which can then be used to determine the constitutive model for the joint under arbitrary loading conditions. In general, Eq. (29) cannot be solved in closed

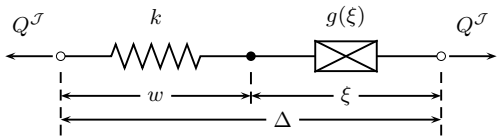

Figure 4: Interface constitutive framework.

form except under specific assumptions regarding the joint response. For example, from Quinn and Segalman the unidirectional loading response g can be expressed as

$$g(\xi) = F_0 \left(\frac{\xi}{\ell_0}\right)^{\frac{\beta}{\beta+1}}, \tag{30}$$

where β is related to the distribution of the frictional intensity (coefficient of friction multiplied by the normal traction) over the interface. Thus Eq. (29) is algebraic but reduces to a quadratic equation only for $\beta = 1$, which corresponds to a uniform frictional intensity.

Note that if $\delta Q = Q^{\mathcal{J}} - Q^{\mathcal{K}}$, the difference between the joint and monolithic force, is small compared to the monolithic force $Q^{\mathcal{K}} = k\,\Delta$, then the term δQ on the right-hand side of Eq. (29) can be neglected, so that

$$g\left(-\frac{\delta Q}{k}\right) \sim k\,\Delta, \quad \longrightarrow \quad \delta Q \sim -k\,g^{-1}(k\,\Delta). \tag{31}$$

For the unidirectional loading given in Eq. (30), this reduces to

$$\delta Q(\Delta) \sim -(k\,\ell_0)\left(\frac{k\,\Delta}{F_0}\right)^{(1+\beta)/\beta}. \tag{32}$$

Therefore the contribution of the interface to the modal equations can be determined for arbitrary loading conditions from this loading curve.

In terms of this expression for δQ, the damped equations of motion can be written as

$$m\,\ddot{A}_1 - (\sqrt{2}-1)\,\delta Q + (2-\sqrt{2})\,k\,A_1 = 0, \tag{33a}$$

$$m\,\ddot{A}_2 - \delta Q + 2\,k\,A_2 = 0, \tag{33b}$$

$$m\,\ddot{A}_3 + (\sqrt{2}+1)\,\delta Q + (2+\sqrt{2})\,k\,A_3 = 0. \tag{33c}$$

In the description of the interface force the displacement across the interface Δ is written as

$$\begin{aligned}\Delta(t) &= u_3(t) - u_2(t)\\ &= \left(1-\sqrt{2}\right)\,A_1(t) + (-1)\,A_2(t) + \left(1+\sqrt{2}\right)\,A_3(t).\end{aligned} \tag{34}$$

Once again, the resulting equations of motion are coupled only through the interface force δQ.

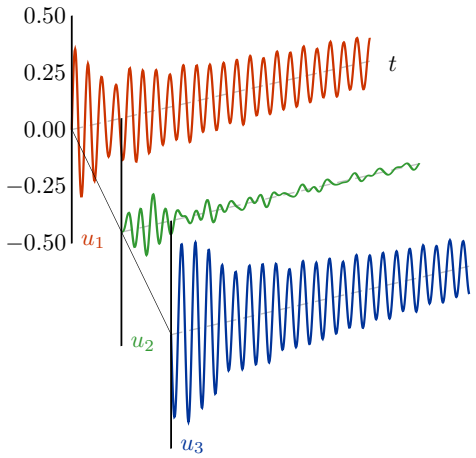

Figure 5: Response of the 3-dof system with a mechanical joint between masses 2 and 3; $0 \le t < 50$. The initial conditions excite only the second mode.

In Figure 5 the numerical simulation of this system is shown with $m = 1.00$ and $k = 4.00$. In addition, the interface parameters are chosen as

$$\beta = 1.00, \quad \ell_0 = 10.00, \quad F_0 = 20.00. \tag{35}$$

At $t = 0$ the conditions of the system are such that the system initially responds in the second mode, so that

$$\begin{aligned} A_1(0) &= 0, \quad A_2(0) = 0, \quad & A_3(0) &= 0,\\ \dot{A}_1(0) &= 0, \quad \dot{A}_2(0) = 1.00, \quad & \dot{A}_3(0) &= 0, \end{aligned} \tag{36}$$

while the interface is initially undeformed. In the figure the response of each mass is shown for $0 \le t < 50$, reconstructed from the equations of motion in modal form. The response of the system decays due to the presence of the dissipation at the mechanical joint. For comparison, if the interface were not present, with these initial conditions the second mass would remain stationary while u_1 and u_3 would move out of phase with identical amplitudes.

In Figure 6 the corresponding hysteresis curve is shown for this response. Recall that δQ represents the difference between the interface force and the force arising from the monolithic structure. Thus the overall shape of the hysteresis curves indicate that overall the joint has a softening effect on the structure as compared to the monolithic system.

The mechanical energy in each mode is defined as

$$\mathcal{E}_i(t) = \frac{\dot{A}_i^2(t)}{2} + \frac{\omega_i^2\,A_i^2(t)}{2}. \tag{37}$$

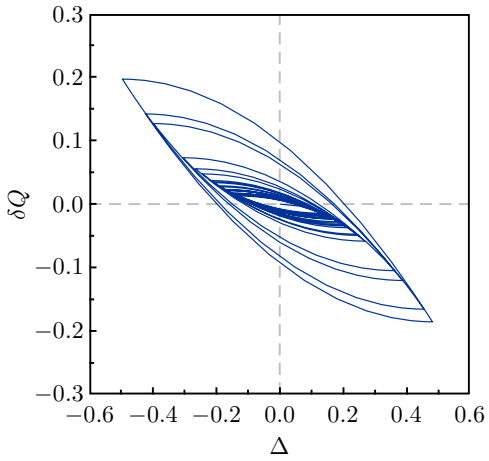

Figure 6: Hysteresis curve.

For the undamped structural system or also one with proportional damping, the modes are uncoupled. In addition, for such systems the modal energy defined above decays exponentially. Even with general viscous damping, as considered in the initial example, the energy decay is, on average, exponential, with slight fluctuations due to the mode coupling. However, with the inclusion of the mechanical joint the energy decay is no longer exponential. However, following recent work by Sapsis et al. [22] an equivalent time-dependent decay rate can be identified through the decay of the energy. For a decoupled mode with damping the modal equation can be written as

$$\ddot{A} + \sigma\,\dot{A} + \omega^2\,A = 0, \tag{38}$$

the mechanical energy decays as

$$\dot{\mathcal{E}}(t) = -\sigma\,\dot{A}^2(t). \tag{39}$$

Define $\langle z \rangle$ as the time-averaged value of z over one cycle of motion, so that

$$\langle z \rangle \equiv \frac{1}{T}\int_0^T z(t)\,dt. \tag{40}$$

For a system with light damping, the mechanical energy varies slowly, so that $\langle \dot{A}^2 \rangle = \langle \omega^2\,A^2 \rangle$ and $\langle \mathcal{E} \rangle = \langle \dot{A}^2 \rangle$. Therefore the average mechanical energy evolves as

$$\langle \dot{\mathcal{E}} \rangle = -\sigma\,\langle \mathcal{E}_i \rangle. \tag{41}$$

For linear damping, the slope of $\log\langle \mathcal{E} \rangle$ when viewed on a log-linear plot is constant and equal to $-\sigma$. In the presence of nonlinear damping, the slope of $\log\langle \mathcal{E} \rangle$ is no longer constant. However, an equivalent instantaneous decay rate of the system can be identified as the instantaneous slope of this plot and σ becomes a function of time. The slope of $\log\langle \mathcal{E} \rangle$ is calculated by fitting a polynomial to this plot to represent the time-average, and then explicitly calculating the derivative.

As seen in Figure 7a, when the evolution of $\mathcal{E}_i$ is shown on a log-linear scale, the decay is not a straight line, as it would be for linear damping. Note that the response is dominated by the second mode so that $\mathcal{E}_2$ is several orders of magnitude larger than that of the remaining modes. Moreover, its decay is relatively smooth, in contrast to the values of $\mathcal{E}_1$ and $\mathcal{E}_3$ which fluctuate due to the additional coupling and energy exchange between the modes.

In Figure 7b the identified exponential decay rate of the second mode, defined as σ_2, is shown versus time. Clearly, the exponential decay rate is not constant. Instead, the equivalent damping decreases with the amplitude of the response. The initial decay of the second mode ($0 < t < 10$) can be attributed in part to the transfer of energy to the (initially) unexcited structural modes, due to the mode coupling introduced by the interface. Then, for longer times ($t > 10$) the damping within the interface becomes the dominant source of the nonlinear energy dissipation.

Several recent efforts to incorporate interfacial damping discretize the mechanical joint [8, 12, 15, 19, 23], including the series-series Iwan modeling on which this approach is based [20]. However, as the minimum length scale of the interface model decreases, the resulting computational effort required for its solution grows. For several of these efforts a reduced-order model is then developed within the interface to reduce the computational effort required by the initial representation of the dissipation. In contrast, this simulation uses the continuum approximation for the interface damping of an elastic rod, and suffers no increase in computational effort arising from time discretization refinement, although in the present model the time at which slip reversals occur must be accurately calculated. In simple tests the monolithic system took 0.86 s of cpu time while the jointed structure required 1.42 s of cpu time for a simulation of 50 time units.

4 CONCLUSIONS

This work has developed a compact form of the equations of motion for structural systems with isolated nonlinearities, when written in terms of the linear modal coordinates. As applied to the problem of a discrete three-mass system as considered by Segalman [19], the formulation is exact, in that once the interface force is known the resulting equations of motion are exact. However, the constitutive be-

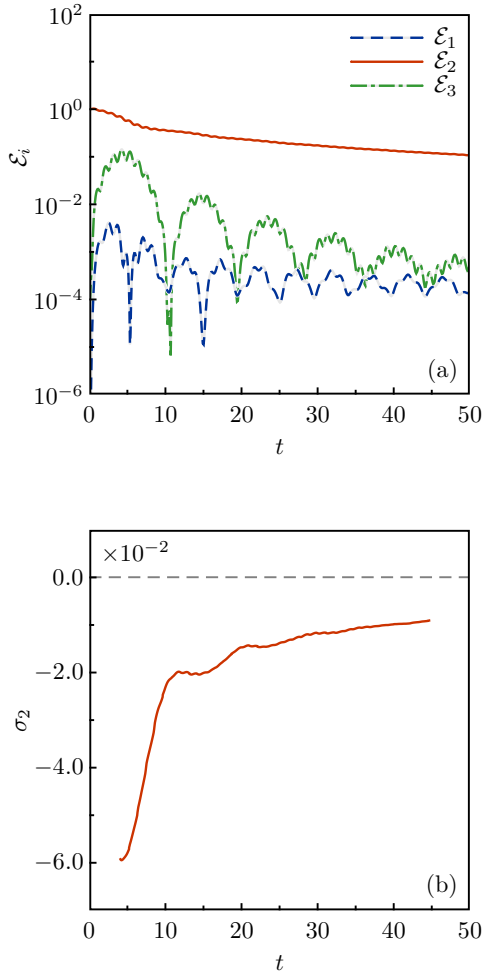

Figure 7: Modal Energy; (a) $\mathcal{E}_i(t)$, (b) Identified exponential decay rate, σ_2.

havior of the interface must still be specified. This step is accomplished referring back to Miller and Quinn [20], in which a two-sided interface model was decoupled into an elastic and dissipative component. In the present work the continuum limit of the dissipative chain, equivalent to a series-series Iwan model, is used together with Masing's hypothesis to describe the role of the mechanical joint on the overall structural response. By relying on the continuum dissipative model, the resulting simulation is computationally efficient and is described in terms of joint parameters that can easily be related back to measurable quantities such as the coefficient of friction.

REFERENCES

[1] E. E. Ungar, The statue of engineering knowledge concerning the damping of built-up structures, J. Sound Vib. 26 (1) (1973) 141–154.

[2] L. Gaul, J. Lenz, Nonlinear dynamics of structures assembled by bolted joints, Acta Mech. 125 (1997) 169–181.

[3] R. A. Ibrahim, C. L. Pettit, Uncertainties and dynamic problems of bolted joints and other fasteners, J. Sound Vib. 279 (3–5) (2005) 857–936.

[4] C. J. Hartwigsen, Y. Song, D. M. McFarland, L. A. Bergman, A. F. Vakakis, Experimental study of nonlinear effects in a typical shear lap joint configuration, J. Sound Vib. 277 (1–2) (2004) 327–351.

[5] H. Ouyang, M. J. Oldfield, J. E. Mottershead, Experimental and theoretical studies of a bolted joint excited by a torsional dynamic load, Intl. J. Mech. Sci. 48 (2006) 1447–1455.

[6] W. Chen, X. Deng, Structural damping caused by micro-slip along frictional interfaces, Intl. J. Mech. Sci. 47 (2005) 1191–1211.

[7] E. Cigeroglu, N. An, C.-H. Menq, Forced response prediction of constrained and unconstrained structures coupled through frictional contacts, J. Eng. Gas. Turb. Power—T. ASME 131 (2009) 022505.

[8] D. J. Segalman, Modelling joint friction in structural dynamics, Struct. Control Health Monit. 13 (2006) 430–453.

[9] D. J. Segalman, Model reduction of systems with localized nonlinearities, J. Comput. Nonlinear Dynam.—T. ASME 2 (3) (2007) 249–266.

[10] L. Heller, E. Foltête, J. Piranda, Experimental identification of nonlinear dynamic properties of built-up structures, J. Sound Vib. 327 (2009) 183–196.

[11] W. D. Iwan, A distributed-element model for hysteresis and its steady-state dynamic response, J. Appl. Mech.—T. ASME 33 (1966) 893–900.

[12] Y. Song, C. J. Hartwigsen, D. M. McFarland, A. F. Vakakis, L. A. Bergman, Simulation of dynamics of beam structures with bolted joints using adjusted Iwan beam elements, J. Sound Vib. 273 (2004) 249–276.

[13] D. D. Quinn, D. J. Segalman, Using series-series Iwan-type models for understanding joint dynamics, J. Appl. Mech.—T. ASME 72 (2005) 778–784.

[14] M. Oldfield, H. Ouyang, J. E. Mottershead, Simplified models of bolted joints under harmonic loading, Comp. Struct. 84 (2005) 25–33.

[15] D. J. Segalman, A four-parameter Iwan model for lap-type joints, J. Appl. Mech.—T. ASME 72 (5) (2005) 752–760.

[16] E. Cigeroglu, W. Lu, C.-H. Menq, One-dimensional dynamic microslip friction model, J. Sound Vib. 292 (2006) 881–898.

[17] T. J. Royston, Leveraging the equivalence of hysteresis models from different fields for analysis and numerical simulation of jointed structures, J. Comput. Nonlinear Dynam.—T. ASME 3 (3) (2008) 031006.

[18] V. Jaumouillé, J.-J. Sinou, B. Petitjean, An adaptive harmonic balance method for predicting the nonlinear dynamic responses of mechanical systems—Application to bolted joints, J. Sound Vib. 329 (19) (2010) 4048—-4067.

[19] D. J. Segalman, A modal approach to modeling spatially distributed vibration energy dissipation, Tech. Rep. SAND2010–4763, Sandia National Laboratories (August 2010).

[20] J. D. Miller, D. D. Quinn, A two-sided interface model for dissipation in structural systems with frictional joints, J. Sound Vib. 321 (2009) 201–219.

[21] D. J. Segalman, M. J. Starr, Inversion of Masing models via continuous Iwan systems, Intl. J. Non-linear Mech. 43 (2008) 74–80.

[22] T. P. Sapsis, D. D. Quinn, A. F. Vakakis, L. A. Bergman, Effective stiffening and damping enhancement of structures with strongly nonlinear local attachments, J. Vib. Acoust.Accepted for publication.

[23] M. Guthrie, D. Kammer, A general reduced representation of one-dimensional frictional interfaces, J. Appl. Mech.—T. ASME 75 (1) (2008) 011019.